Journal of Applied Science, Engineering, Technology and Management
Vol. 04, Issue 1, June 2026 pp. 09–12

# Planar Sub-THz Bandpass Filter Based on a Cross-Arrow Slot FSS for Radar and Secure Communication Applications

Anitha George
*School of Engineering*
*Cochin University of Science and Technology*
*Cochin, Kerala, India*
anithageorge@cusat.ac.in

Abdulla P
*School of Engineering*
*Cochin University of Science and Technology*
*Cochin, Kerala, India*
abdulla@cusat.ac.in

Nabeel A M
*School of Engineering*
*Cochin University of Science and Technology*
*Cochin, Kerala, India*
22ec062nabe@ug.cusat.ac.in

Pranav P R
*School of Engineering*
*Cochin University of Science and Technology*
*Cochin, Kerala, India*
22ec069pran@ug.cusat.ac.in

***Abstract*—A cross-arrow slot frequency selective surface (FSS) is proposed for sub-terahertz (sub-THz) bandpass filtering, offering enhanced spectral performance over conventional cross-shaped designs. Full-wave simulations in CST Studio Suite demonstrate a sharp transmission peak (S21) of −0.3 dB at 0.175 THz, with a −10 dB bandwidth of 25 GHz and a quality factor (Q) of 6.5. The design achieves excellent impedance matching, as indicated by a reflection coefficient (S11) of −37 dB. The arrow-shaped slot extensions promote strong current confinement, resulting in high spectral selectivity and low insertion loss. Parametric tuning enables resonance shifting across the 0.15 THz – 0.25 THz range, covering a wide portion of the sub-THz spectrum. All simulations were done in the CST microwave suite, and the results were validated in HFSS software. The proposed filter is also suitable for military sub-THz systems, including secure high-data-rate communication links, radar front-ends, and spectrum-selective sensing applications.**

***Keywords Terms*—*Cross Arrow slot, Frequency selective surface, Sub Terahertz.***

## I. Introduction

The sub-terahertz (sub-THz) band (0.1–0.3 THz) is of increasing importance in applications including high-speed wireless communication, biomedical imaging, and spectroscopic sensing [1], [2]. Within these systems, bandpass filters are essential for isolating narrow frequency bands while maintaining low insertion loss and strong out-of-band rejection. Frequency Selective Surfaces (FSS) offer a compact and planar solution for implementing such filters and are compatible with standard lithographic techniques [3].

Among common FSS geometries, cross-slot-based designs have been widely used due to their polarization independence and structural simplicity [4], [5]. However, these designs typically exhibit limited Q-factors, moderate spectral selectivity, and restricted tunability in the sub-THz range. Previous studies have shown that current distribution in simple cross structures lacks strong confinement, leading to reduced impedance matching [6].

Recent developments have explored alternatives such as Jerusalem cross structures, dielectric-loaded FSS, and modified slot geometries [7]– [10] to overcome the limitations of conventional structures. While these approaches improve impedance matching and bandwidth control, they often compromise insertion loss.

In this work, a cross-arrow slot-based FSS is proposed for efficient sub-THz bandpass filtering. The arrow-shaped terminations enhance current localization at the slot tips, resulting in a sharper resonance and higher spectral selectivity. Full-wave simulations using CST Studio Suite show a reduced insertion loss of 0.3 dB, perfect impedance matching with a reflection coefficient of −37 dB, and −10 dB bandwidth of 25 GHz, at a resonant frequency of 0.175 THz, corresponding to a Q-factor of 6.5. The filter also supports parametric tuning of the resonance across 0.15 THz–0.25 THz, enabling versatile application in adaptive sensing, imaging, and wireless THz systems.

The selected center frequency around 0.175 THz and the moderate bandwidth of 25 GHz fall within a sub-THz window that is particularly attractive for defense applications, as it enables high-resolution radar sensing, reduced antenna size, and secure short-range high-data-rate communication while maintaining manageable atmospheric attenuation [1], [2].

## II. Design and Simulation

The unit cell structure and geometric parameters of the proposed cross-arrow slot-based sub-terahertz bandpass filter is illustrated in Fig. 1. The periodicity of the unit cell, $p$ is set to 1000 $\mu$m, ensuring adequate spatial separation for minimizing inter-cell coupling. The polyimide substrate has a thickness, $h = 20$ $\mu$m, providing mechanical support while maintaining low dielectric loss with a relative permittivity of 3.5 and a loss tangent of 0.005. The frequency-selective pattern is etched into gold layer with thickness $t = 5$ $\mu$m, and conductivity of $\sigma = 4.1\text{x}10^7$ S/m deposited on the substrate, resulting in minimal ohmic losses and ensuring excellent electrical performance at terahertz frequencies.

The central radiating feature is a cross-slot structure, where $l$ and $w$ represent its length and width, respectively. The design incorporates an arrow-like extension at the end of the cross

eISSN 2584-0371


Received for review: 22-04-2026
Accepted for publication: 04-05-2026
Published: 15-05-2026

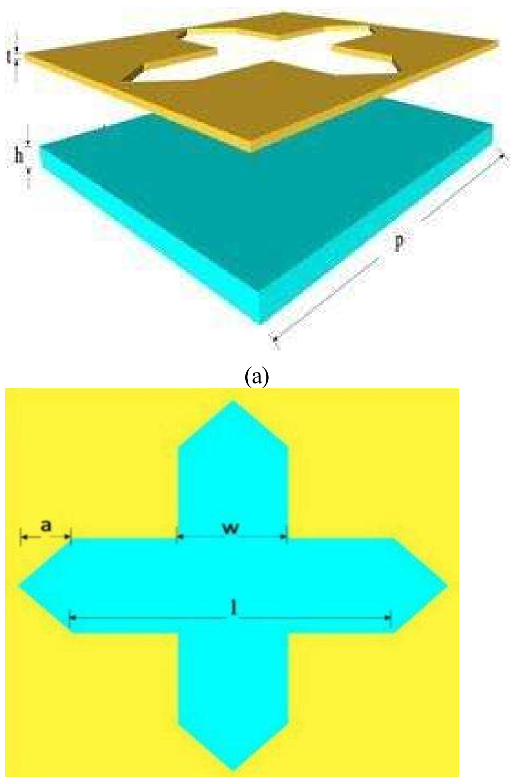


(a)

(b)

Fig. 1: Proposed cross-arrow slot FSS: (a) unit cell geometry showing dimensional parameters, (b) three-dimensional layered configuration.

slot, with a length, $a = 119\ \mu$m, which enhances the current distribution and electric field confinement, contributing higher quality factor and improved selectivity.

The resulting S-parameter characteristics, shown in Fig. 2, confirm a bandpass response at 0.175 THz, with −10 dB bandwidth of 25 GHz, insertion loss of 0.3 dB, and reflection coefficient, $S_{11}$ of –37 dB. The values of length and width chosen were $l = 700\ \mu$m and $w = 240\ \mu$m. To validate the simulated results the designed structure is simulated in ANSYS HFSS, demonstrating excellent agreement and confirming the reliability of the proposed structure for sub-THz filtering applications.

The use of the cross-arrow slot geometry enables functionalities that are difficult to realize with conventional cross-slot FSS filters at sub-terahertz frequencies. In a standard cross-slot structure, limited current confinement and moderate quality factor restrict the achievable spectral selectivity, making it unsuitable for narrowband, interference-critical military systems. By introducing arrow-shaped terminations, the proposed geometry significantly enhances current localization and effective electrical length, allowing a sharp bandpass response at a center frequency of 0.175 THz with a controlled bandwidth of 25 GHz. This combination enables highly selective sub-THz filtering while maintaining low insertion loss, which is essential for short-range high-resolution surveillance radar

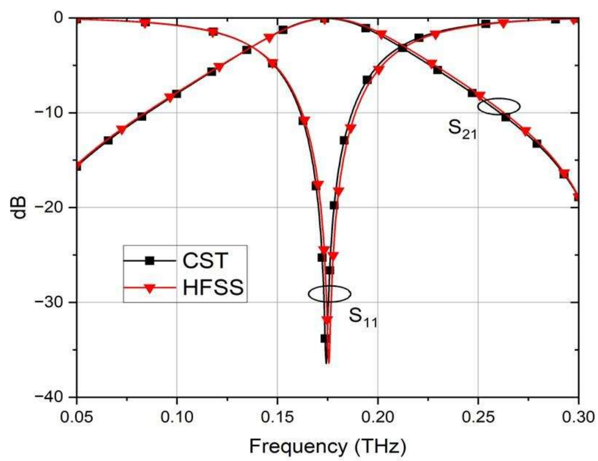


Fig. 2: Comparison of simulated S-parameters ($S_{11}$ and $S_{21}$) from CST and HFSS for the proposed structure.

used for target identification and threat discrimination on unmanned aerial and ground platforms. Such radar systems require narrowband operation to suppress clutter and jamming while operating at higher frequencies for improved spatial resolution capabilities [1], [9]. Therefore, the cross-arrow slot FSS uniquely supports compact, high-selectivity sub-THz radar front-ends for military surveillance and sensing applications that are beyond the practical performance limits of normal cross-slot geometries.

## III. Equivalent Circuit Analysis

The proposed cross-arrow slot FSS can be modeled using an equivalent circuit approach to provide physical insight into its electromagnetic behavior as shown in Fig. 3. Since the structure consists of a slot etched on a metallic surface, it behaves as a magnetic dipole and is therefore represented by a shunt parallel LC resonator connected across a transmission line. The transmission line models the propagation of electromagnetic waves in free space and through the dielectric substrate, while the LC resonator captures the reactive behavior of the slot geometry. The dielectric substrate is modeled as a transmission line section characterized by its relative permittivity and thickness, which introduces additional phase delay and modifies the effective impedance seen by the incident wave.

The inductance in the equivalent circuit arises from the surface current flowing along the arms of the cross-arrow slot, while the capacitance is mainly due to the electric field coupling across the slot gaps and fringing effects, particularly at the sharp edges of the arrow tips. These sharp edges enhance the local electric field concentration, thereby increasing the effective capacitance. The resonance behavior of the structure is governed by the interaction between these inductive and capacitive effects. At resonance, the parallel LC circuit exhibits high impedance, which minimizes the shunt admittance and reduces the power diverted from the forward transmission path. This condition allows maximum electromagnetic energy to

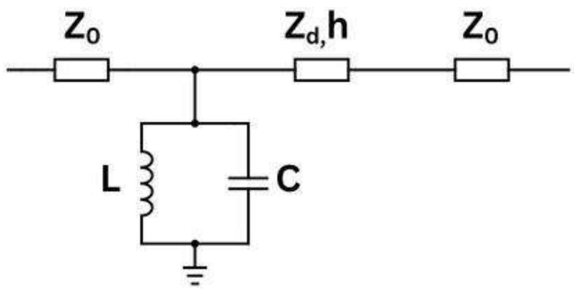


Fig. 3: Equivalent circuit model of the proposed FSS.

transmit through the structure, thereby producing the observed bandpass response. Away from resonance, the LC circuit impedance decreases and the shunt admittance increases, causing greater energy diversion and a corresponding reduction in transmission.

The resonant frequency of the equivalent circuit can be

$$f_0 = \frac{1}{2\pi\sqrt{LC}} \quad (1)$$

Furthermore, the characteristic impedance of the dielectric substrate modeled as a transmission line is given by

$$Z = \frac{Z_0}{\sqrt{\varepsilon_r}} \quad (2)$$

From the equivalent circuit perspective, it is evident that the resonant frequency can be tuned by modifying the geometrical parameters of the unit cell. An increase in the slot length leads to higher inductance, while a decrease in the gap between slot edges increases capacitance. Similarly, an increase in the dielectric constant of the substrate enhances the effective capacitance, thereby shifting the resonant frequency toward lower values. Thus, the equivalent circuit model provides a simple yet powerful tool for analyzing and designing the proposed FSS structure.

## IV. Parametric Study

Two parametric evaluations were carried out by altering the cross-slot's width and length to investigate how geometric parameters impact the suggested filter's performance. Firstly, all other dimensions remain constant while varying length $l$. The simulated transmission response in this instance is shown in Fig. 4. The reflection response shows a downward shift in resonance frequency as $l$ increases, which is explained by an increase in electrical length and effective inductance. For $l$ = 500 $\mu$m, 600 $\mu$m, and 700 $\mu$m, the 10-dB bandwidths are 15 GHz at 0.22 THz, 20 GHz at 0.2 THz, and 25 GHz at 0.175 THz, respectively. The insertion loss is likewise modest in all the combinations, at about −0.3 dB. Excellent impedance matching is indicated by the reflection coefficients of −32 dB, −34 dB, and −36 dB, respectively.

Furthermore, it is shown that the Q-factor and VSWR do not significantly degrade when l is reduced up to 300 μm

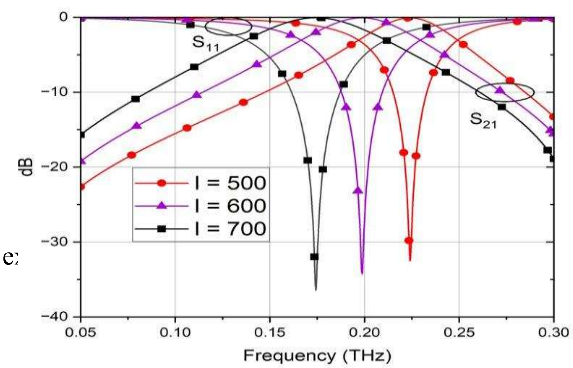


Fig. 4: Parametric analysis of the bandpass filter with vary-ing cross lengths: Transmission (S21) and reflection (S11) responses

Accordingly, S11 achieves a −30 dB value at a centre frequency of 0.25 THz with a −10 dB bandwidth of 12 GHz. The structural geometry is affected by an increase in l above 700 μm..

Secondly, as illustrated in Fig. 5, the slot width, $w$, systematically varied throughout 170 $\mu$m to 310 $\mu$m while maintaining all other parameters constant. In both transmission and reflection properties, a rise in $w$ causes a discernible change of the resonance frequency towards higher values. All configurations maintain an insertion loss of 0.3 dB, confirming acceptable impedance matching. Wider slots broaden the bandwidth, as seen by the −10 dB bandwidths for $w$ = 170 $\mu$m, 240 $\mu$m, and 310 $\mu$m, which are 20 GHz, 25 GHz, and 35 GHz for the centre frequencies of 0.16 THz, 0.17 THz, and 0.18 THz, respectively. Better return loss characteristics are demonstrated by reflection coefficients of −35 dB, −36.5 dB, and −37 dB, which guarantee effective signal transmission.

Without affecting the structural geometry or important performance metrics, the slot width, $w$, can be changed from a minimum of 100 $\mu$m, which results in a −10 dB bandwidth of 15 GHz at 0.15 THz, to a maximum of 400 $\mu$m, which results in a −10 dB bandwidth of 40 GHz at 0.2 THz.

## V. Results and Discussions

Full-wave electromagnetic simulations in CST Studio Suite are used to build the suggested cross-arrow slot frequency selective surface. There is a bandpass response in the structure. By altering the filter's cross arm's width or length, the resonant frequency can be adjusted. It has been found that the resonance frequency may be adjusted from 0.17 THz to 0.25 THz with almost constant bandwidth by changing length, $l$ from 700 $\mu$m to 300 $\mu$m. Similarly, the resonant frequency can be changed from 0.15 THz to 0.2 THz by changing the width, $w$ from 100 $\mu$m to 400 $\mu$m.

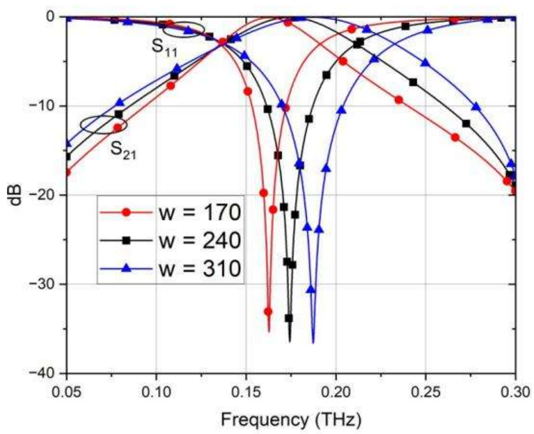


Fig. 5: Parametric analysis of the bandpass filter with varying cross widths: Transmission (S21) and reflection (S11) responses.

TABLE I: Comparison of Proposed Design with Existing Sub-THz Filters

| Ref | $f_c$ (THz) | BW (GHz) | RL (dB) | IL (dB) | VSWR |
|---|---|---|---|---|---|
| [11] | 0.24 | 20 | 23 | 0.6 | 1.25 |
| [12] | 0.19 | 24 | 21 | 0.8 | 1.48 |
| [13] | 0.16 | 18 | 19 | 0.5 | 1.31 |
| [14] | 0.28 | 21 | 22 | 1.0 | 1.50 |
| [15] | 0.22 | 23 | 28 | 0.4 | 1.71 |
| **Proposed work** | **0.17** | **25** | **37** | **0.3** | **1.03** |

$f_c$ – Centre Frequency; BW – Bandwidth; RL – Return Loss; IL – Insertion Loss.

The bandwidth is increasing in this instance. From these two observations, the filter can be realized between 0.15 THz to 0.25 THz, choosing the desired values of $l$ and $w$.

With a Q factor of 6.5 and a corresponding voltage standing wave ratio of 1.03 for the optimized filter with $l = 700$ $\mu$m and $w = 240$ $\mu$m, the filter is confirmed to be suitable for high-efficiency sub-terahertz applications. As length increases, the resonance frequency decreases, which is explained by higher inductive loading. Additionally, because of changed current routes and less inductive confinement, wider slots result in higher resonance frequencies and bandwidths. These findings demonstrate that, without sacrificing spectral efficiency, the structure permits accurate geometric tuning control over the resonant frequency. The ideal arrow slot length, which is an extension of the traditional cross structure, is 119 $\mu$m to attain a low VSWR and an improved Q-factor. The suggested filter is compared to other previously published sub-THz bandpass filters [11]– [15] as shown in Table I.

In particular, the cross-arrow slot geometry enables a level of spectral selectivity and impedance matching at 0.175 THz that is difficult to achieve with conventional FSS designs. The controlled 25 GHz bandwidth and sharp resonance make the proposed filter especially suitable for compact sub-THz military radar and surveillance systems, where narrowband operation, interference suppression, and high detection accuracy are critical. These features position the cross-arrow slot FSS as a practical and application-driven solution for advanced military sensing and secure communication front-ends.

## VI. Conclusion

For sub-terahertz applications, a compact and highly effective bandpass filter based on a cross-arrow slot frequency selective surface has been created and examined in this work. CST Studio Suite is used to model the structure, while ANSYS HFSS is used for validation. Good impedance matching is indicated by the passband reflection of −37 dB and a VSWR of 1.03, which validates effective signal transmission. By altering the slot arm length and width, parametric analysis is carried out, demonstrating that exact resonance tuning is possible without sacrificing spectral performance. Finally, the comparison with existing sub-THz filters shows that the suggested cross-arrow slot construction maintains planar configuration while offering better performance. Because of its low insertion loss and adaptable design, this simple FSS is ideal for terahertz applications like spectroscopy, imaging, and next generation wireless communication systems.

## References

[1] M. Tonouchi, "Cutting-edge terahertz technology," *Nature Photonics*, vol. 1, no. 2, pp. 97–105, 2007.

[2] B. Ferguson and X.-C. Zhang, "Materials for terahertz science and technology," *Nature Materials*, vol. 1, no. 1, pp. 26–33, 2002.

[3] N. Engheta and R. W. Ziolkowski, *Metamaterials: Physics and Engineering Explorations*. Hoboken, NJ, USA: Wiley-IEEE Press, 2006.

[4] H. Tao, N. I. Landy, C. M. Bingham, X. Zhang, R. D. Averitt, and W. J. Padilla, "A metamaterial absorber for the terahertz regime: Design, fabrication and characterization," *Optics Express*, vol. 16, no. 10, pp. 7181–7188, 2008.

[5] L. Lu, S. Chen, Q. Wen, and Y. Liu, "A tunable terahertz bandpass filter based on a cross-slot frequency selective surface," *Optics Communications*, vol. 487, p. 126835, 2021.

[6] A. Ferraro, G. Gennarelli, G. Riccio, F. Soldovieri, and R. Pierri, "Characterization of planar metasurfaces with cross-shaped resonators for THz sensing," *IEEE Trans. Terahertz Sci. Technol.*, vol. 7, no. 3, pp. 304–311, May 2017.

[7] H. Yang, C. Lin, Z. Zhu, and Y. Ma, "Modified Jerusalem cross metasurface for terahertz bandpass filtering," *IEEE Access*, vol. 10, pp. 14578–14585, 2022.

[8] A. Shahounv and and M. H. Fard, "Design of a high-performance single-layer bandpass frequency selective surface for terahertz applications," *AEU¨ Int. J. Electron. Commun.*, vol. 116, p. 153049, 2020.

[9] I. Komarov and A. Meshchanov, "High-Q terahertz bandpass filter based on symmetric arrow-slot metasurface," *Sensors Actuators A: Phys.*, vol. 358, p. 114282, 2024.

[10] Y. Yu, H. Yang, and Z. Fan, "Investigation of dielectric-loaded metasurfaces for tunable sub-terahertz filters," *IEEE Access*, vol. 12, pp. 30055–30063, 2024.

[11] M. A. Alharthi *et al.*, "Design of a compact sub-THz bandpass filter using complementary split-ring resonators," *IEEE Access*, vol. 11, pp. 7568–7575, 2023.

[12] X. Zhang *et al.*, "Nested slot metasurfaces for tunable terahertz filters," *Microw. Opt. Technol. Lett.*, vol. 65, no. 12, pp. 1224–1230, 2023.

[13] Y. H. Kim and J. Park, "Gap-tuned cross dipole filters for sub-terahertz applications," *IEEE Trans. Compon. Packag. Manuf. Technol.*, vol. 12, no. 6, pp. 889–896, 2022

[14] R. Chen *et al.*, "High-Q dielectric-loaded terahertz filter based on metasurface design," *Sensors Actuators A: Phys.*, vol. 347, p. 113938, 2022

[15] T. Lin *et al.*, "A bowtie slot-based THz bandpass filter with enhanced stopband rejection," *J. Infrared Millim. Terahertz Waves*, vol. 44, pp: 241-253, 2023.